

An independent endocytic pathway stimulates different monocyte subsets by the $\alpha 2$ N-terminus domain of vacuolar-ATPase

Christina Kwong, Alice Gilman-Sachs & Kenneth Beaman

To cite this article: Christina Kwong, Alice Gilman-Sachs & Kenneth Beaman (2013) An independent endocytic pathway stimulates different monocyte subsets by the $\alpha 2$ N-terminus domain of vacuolar-ATPase, OncoImmunology, 2:1, e22978, DOI: [10.4161/onci.22978](https://doi.org/10.4161/onci.22978)

To link to this article: <https://doi.org/10.4161/onci.22978>



Copyright © 2013 Landes Bioscience



View supplementary material [↗](#)



Published online: 01 Jan 2013.



Submit your article to this journal [↗](#)



Article views: 275



View related articles [↗](#)



Citing articles: 8 View citing articles [↗](#)

An independent endocytic pathway stimulates different monocyte subsets by the a2 N-terminus domain of vacuolar-ATPase

Christina Kwong, Alice Gilman-Sachs and Kenneth Beaman*

Department of Microbiology and Immunology; Chicago Medical School; Rosalind Franklin University of Medicine and Science; Chicago, IL USA

Keywords: cancer-related inflammation, CD14, CD16, IL-1, pro-inflammatory monocytes, tumor associated macrophages, vacuolar ATPase

Abbreviations: a2NTD, N-terminus domain of the a2 isoform vacuolar ATPase; a2V, a2 isoform vacuolar ATPase; CRI, cancer-related inflammation; TAM, tumor-associated macrophage; V-ATPase, vacuolar ATPase

The vacuolar ATPase (V-ATPase) plays an important role in tumor progression and metastases. A novel peptide from the a2 isoform of V-ATPase called a2NTD has been shown to exert an immunoregulatory role in the tumor microenvironment by controlling the maturation of monocytes toward a tumor-associated macrophage phenotype. Our data indicate that a2NTD binds to the surface of monocytes. a2NTD was preferentially endocytosed by pro-inflammatory monocytes bearing a CD14⁺CD16⁺ phenotype, which is associated with the monocyte-to-macrophage maturation process. Both a2NTD binding and internalization led to production of the pro-inflammatory cytokines interleukin (IL)-1 α and IL-1 β by CD14⁺CD16⁻ (classical) and CD14⁺CD16⁺ (intermediate) monocytes. a2NTD was internalized via a macropinocytosis mechanism utilizing scavenger receptors. However, the inhibition of a2NTD endocytosis did not reduce cytokine production by monocytes. This points to the existence of two receptors that respond to a2NTD: scavengers receptors that mediate cellular uptake and an hitherto unidentified receptor stimulating the production of inflammatory cytokines. Both of these monocyte receptors may be important in generating the localized inflammation that is often required to promote tumor growth and hence may constitute novel targets for the development of anticancer drugs.

Introduction

Vacuolar ATPases (V-ATPases) are multi-protein complexes found on the surface of tumor cells.^{1,2} V-ATPases impact on tumorigenesis at they acidify the extracellular environment via their proton pumping activity. This enables the maturation of pH-sensitive degradative enzymes such as matrix metalloproteinases (MMPs), which promote tumor metastasis.^{3,4} Increased cell surface expression of V-ATPases has indeed been linked to tumor cell invasion.⁵

Tumor cells secrete cytokines and other proteins that dictate various facets of the immune response that they will generate, including the activation and polarization of specific macrophage and neutrophil subsets.^{6,7} Cytokines such as interferon γ (IFN γ) skew macrophages toward a classically activated phenotype called M1, which participates in tumor destruction. In contrast, cytokines such as interleukin (IL)-4, IL-13 and IL-10 promote the maturation of alternatively activated M2 macrophages.^{8,9} The M2 phenotype promotes tumor survival by favoring proliferation and tumor progression,¹⁰ as well as by stimulating angiogenesis

and lymphangiogenesis.¹¹ M2 macrophages promote extracellular matrix remodeling¹² while at the same time regulating a complex chemokine network.¹³

Blood monocytes are generally viewed as a heterogeneous population of cells that constitute the precursors to tissue macrophages. Monocytes are differentiated based on the cell surface expression of two markers: the lipopolysaccharide (LPS)-binding protein CD14 and the Fc γ receptor CD16. In 2010, the nomenclature was modified to include three subtypes of monocytes based on these two markers. Classical monocytes display a CD14⁺CD16⁻ phenotype and represent 80-90% of all monocytes. The minor populations consist of CD14⁺CD16⁺ (intermediate) and CD14⁺CD16⁺⁺ (non-classical) monocytes.¹⁴ Monocytes expressing both CD14 and CD16 show a more mature morphological and functional phenotype than their CD16⁻ counterparts and are thought to constitute the specific precursors of tissue-resident macrophages.¹⁵ Our studies use this new classification system, however many of the references use the old nomenclature and so will be referred to as originally published.

*Correspondence to: Kenneth Beaman; Email: kenneth.beaman@rosalindfranklin.edu

Submitted: 07/04/12; Revised: 11/19/12; Accepted: 11/20/12

<http://dx.doi.org/10.4161/onci.22978>

Citation: Kwong C, Gilman-Sachs A, Beaman K. An independent endocytic pathway stimulates different monocyte subsets by the a2 N-terminus domain of vacuolar-ATPase. *Oncolimmunology* 2013; 2:e22978

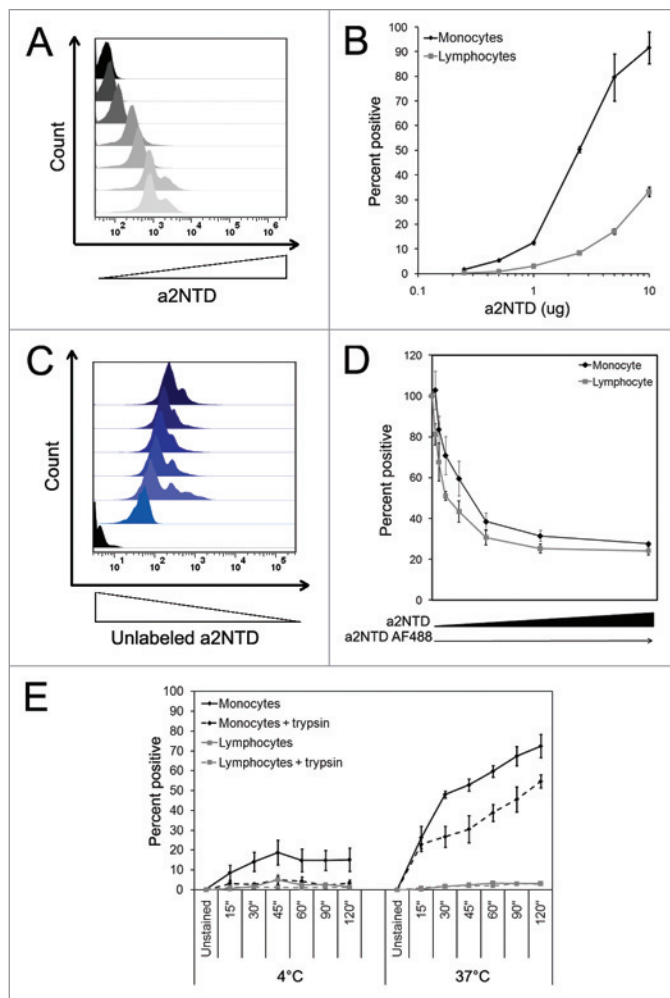


Figure 1. Binding and entry of a2NTD in monocytes and lymphocytes. **(A and B)** Peripheral blood mononuclear cells (PBMCs) fixed with paraformaldehyde were incubated with 0.1–10 $\mu\text{g/mL}$ a2NTD conjugated to Alexa Fluor 488 (a2NTD-AF488). Cell populations were gated based on forward/side scatter. Representative histograms showing a2NTD-AF488 binding in monocytes are presented in **(A)**; the black peak refers to unstained cells. In **(B)**, the percentage of a2NTD binding to monocytes and lymphocytes is shown (means \pm SEM, $n = 4$). **(C and D)** PBMCs fixed with paraformaldehyde were incubated with 0.1–10 $\mu\text{g/mL}$ unconjugated a2NTD and then with 2 $\mu\text{g/mL}$ a2NTD-AF488. A representative histogram showing competitive inhibition of a2NTD binding to monocytes is reported in **(C)**; the black histogram refers to unstained cells. In **(D)**, the percentages of monocytes and lymphocytes positive for a2NTD binding after competitive assay are shown. Values were normalized to cells that did not receive unlabeled a2NTD. (means \pm SEM, $n = 4$). **(E)** PBMCs were incubated with a2NTD-AF488 for indicated time at 4°C and 37°C. Some of the samples were then treated with 0.1% trypsin-EDTA (dashed lines) for 5 min to remove surface bound a2NTD. Cell populations were analyzed by flow cytometry, upon gating on CD14⁺ events. (means \pm SEM, $n = 8$). The percentage of positive monocytes (black lines) or lymphocytes (gray lines) after a2NTD-AF488 incubation is reported.

kinetics. In addition, a2NTD was preferentially endocytosed by CD14⁺CD16⁺ monocytes and these cells produced high levels of pro-inflammatory cytokines IL-1 α , IL-1 β and tumor necrosis factor α (TNF α), as compared with CD14⁺CD16⁻ monocytes. The endocytosis of a2NTD occurred via a macropinocytosis mechanism that required actin filament and microtubule polymerization. Blocking a2NTD endocytosis had no effects on the intracellular levels of IL-1. Taken together, these data suggest that a2NTD stimulates monocytes to generate pro-inflammatory cytokines via a receptor-mediated mechanism. This putative receptor represents a potential point of intervention that can be further investigated to prevent the maturation of M2 tumor-associated macrophages (TAMs).

Results

a2NTD binds and enters monocytes in a dose- and temperature-dependent manner. The binding of a2NTD was investigated in PBMCs using a fluorescently labeled variant of the peptide. a2NTD bound monocytes in a dose-dependent manner (Fig. 1A). At the highest concentrations of a2NTD, approximately 90% of monocytes were found to interact with a2NTD (Fig. 1B). Lymphocytes were also examined, exhibiting minimal binding of a2NTD, though at the highest concentration of a2NTD tested approximately 30% of lymphocytes were positive (Fig. 1B). Binding specificity was tested in a competition assay. Unlabeled a2NTD was able to compete out the binding of fluorescent a2NTD in both monocytes (Fig. 1C and D) and lymphocytes (Fig. 1D).

Many cellular functions including receptor-mediated internalization are inhibited at 4°C, implying that these conditions

Recently, we have demonstrated a novel role for the a2 isoform of V-ATPase (a2V) in tumor progression. Thus, the N-terminal region of a2V expressed at the plasma membrane of human tumor cells can be cleaved, resulting in the release of a peptide that activates immune cells.¹⁶ When incubated with peripheral blood mononuclear cells (PBMCs), this peptide (a2NTD) causes monocytes to produce IL-1 β .^{17,18} A more detailed investigation revealed that a2NTD induces primary monocytes to develop an IL-12^{low}IL-23^{low}IL-10^{high} M2-like phenotype.¹⁶ Thus, a2NTD was the first cytokine-like factor described to induce the alternative activation pathway in macrophages.

In the present study, we examined the interaction of a2NTD with human monocytes. In particular, we determined binding specificity, which particular monocyte subset is targeted, the mode of cellular entry and the receptors involved. a2NTD bound to monocytes and binding could be competed out with unlabeled peptide. a2NTD was internalized by monocytes and THP-1 cells, though the latter demonstrated slower uptake

Figure 2 (see following page). Temperature-dependent binding and internalization of a2NTD by monocytes. **(A–D)** Peripheral blood mononuclear cells (PBMCs) were pre-incubated at 4°C or 37°C for 30 min, followed by the addition of 10 $\mu\text{g/mL}$ a2NTD conjugated to Alexa Fluor 488 (a2NTD-AF488) for 1 h and staining with an anti-CD14 PE-Texas red antibody for 30 min. Some of the samples were treated with 0.1% trypsin after a2NTD-AF488 incubation to remove surface bound a2NTD. Cells were then placed on slides using a cytospin and imaged using a Nikon fluorescent microscope. Representative images from three independent experiments are shown: PBMCs incubated at 4°C, followed **(A)** or not **(B)** by trypsin treatment; PBMC incubated at 37°C, followed **(C)** or not **(D)** by trypsin treatment.

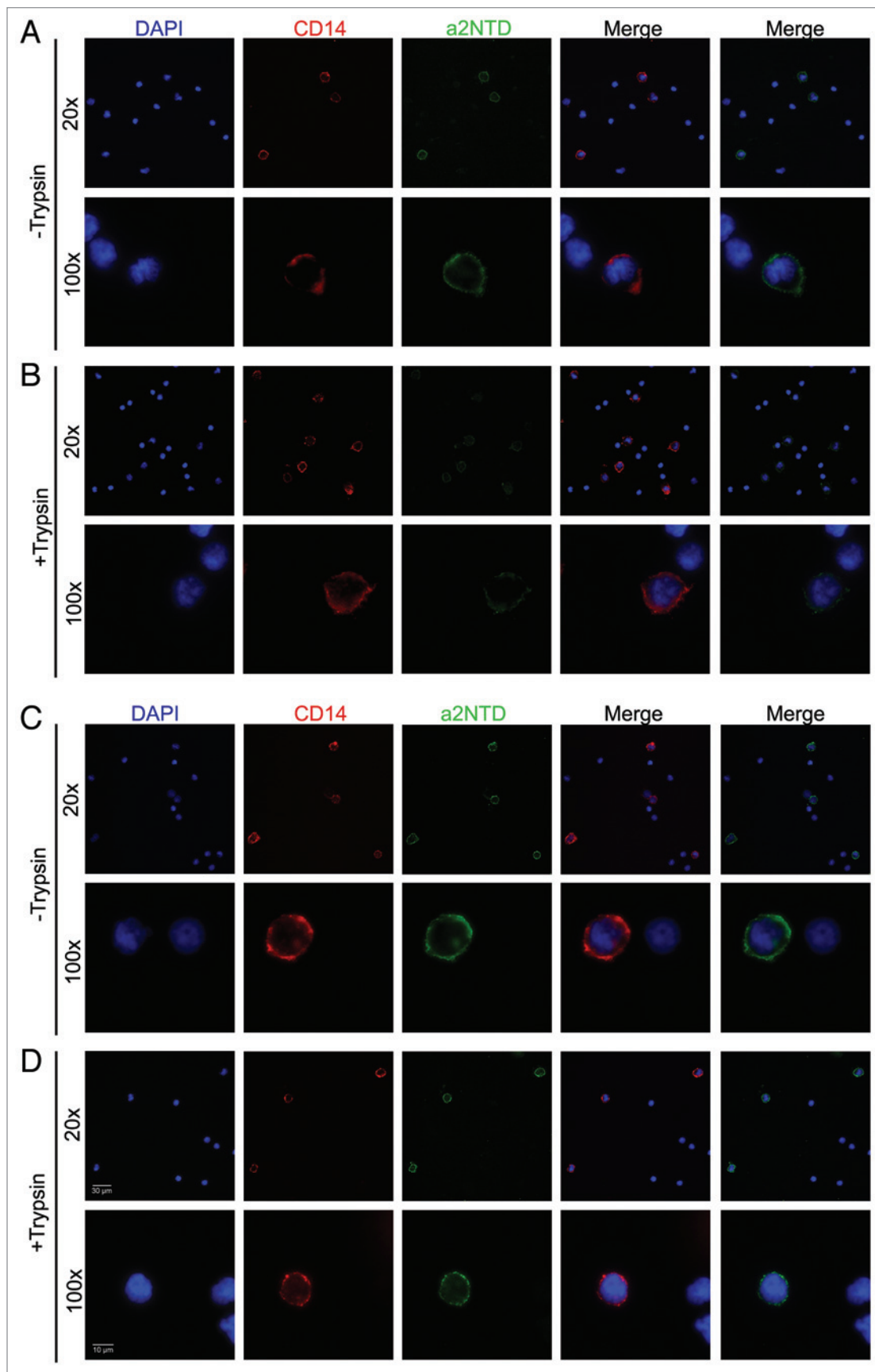


Figure 2. For figure legend, see page e22978-2.

are ideal for studying binding in the absence of internalization. Conversely, both binding and internalization can occur at 37°C.¹⁹ The temperature-dependent binding of fluorescent a2NTD to PBMC was determined at 4°C and 37°C, to confirm an internalization mechanism. There were more a2NTD-positive monocytes, as assessed by flow cytometry, at 37°C (75%)

maintained at 4°C displayed reduced surface fluorescence (Fig. 2B). In comparison, trypsin-treated cells cultured at 37°C exhibited a reduced surface staining but maintained the punctuate intracellular staining (Fig. 2D). To eliminate non-specific phagocytosis as a mechanism of cellular uptake, neutrophils were separately examined. Neutrophils demonstrated much

less endocytosis of a2NTD than monocytes, but slightly more than lymphocytes (Fig. S1). Finally, the monocytic leukemia cell line THP-1 was also examined. While the uptake trend is similar in THP-1 cells and monocytes, the kinetics are much slower for the former. Indeed, after 2h at 37°C, only 17% of THP-1 cells were positive as compared with almost 75% of monocytes (Fig. 1E and Fig. S2).

Endocytosis of a2NTD is energy-dependent and requires structural proteins. In general, filamentous actin is required for receptor-mediated endocytosis.²⁰ The requirement for microtubules depends on the specific receptor that is involved. For example, the inhibition of microtubules blocks complement receptor-mediated, but not Fc receptor-mediated, particle internalization.^{21,22} Moreover, the addition of microtubule-depolymerizing agents such as nocodazole slows down adsorptive and fluid-phase endocytosis.^{23,24} In order to determine if actin or microtubules are important for a2NTD internalization, PBMCs were cultured with a2NTD in presence of cytochalasin D (CytoD), to inhibit F-actin filaments, and colchicines, to inhibit microtubules.

Monocytes demonstrated a greater uptake of a2NTD as compared with a negative control peptide. The pretreatment of PBMCs with inhibitors of actin and microtubules resulted in decreased fluorescence, demonstrating an inhibition of a2NTD uptake (Fig. 3A). Both inhibitors significantly reduced a2NTD entry by approximately 80% as compared with control cells (Fig. 3B and C). Actin and tubulin monomers are in the active state for polymerization when bound to ATP and GTP respectively. The pretreatment of PBMCs with metabolic inhibitors such as sodium azide and 2-deoxyglucose (that

deplete the intracellular ATP pool) or mycophenolic acid (that depletes the pool of GTP) also decreased the uptake of a2NTD (Fig. 3D).

Uptake of a2NTD by monocyte subsets. To determine if different monocyte subsets preferentially internalize a2NTD, monocytes were stained for the surface markers CD14 and CD16 after incubation with a2NTD. CD14⁺⁺CD16⁻ cells constitute the majority of all monocytes, while CD14⁺⁺CD16⁺ and CD14⁺CD16⁺⁺ represent two minor subpopulations.²⁵ We were able to retrieve these three populations by flow cytometry (Table 1). Of note, nearly 100% of CD14⁺⁺CD16⁺ monocytes were positive for a2NTD endocytosis, as compared

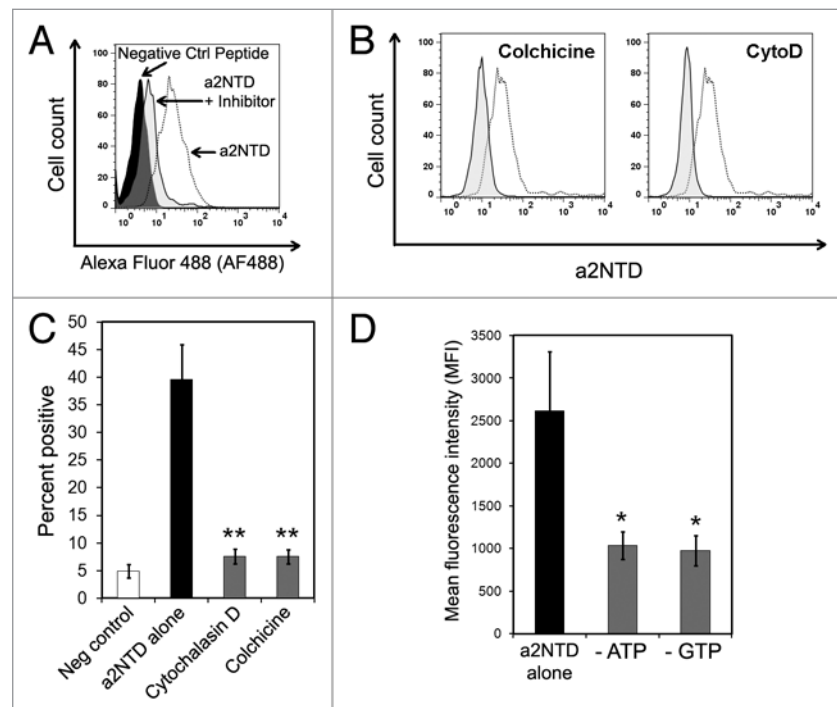


Figure 3. The internalization of a2NTD requires actin, microtubules and an energy source. (A) Representative histogram showing peripheral blood mononuclear cells (PBMCs) incubated with a control peptide, a2NTD conjugated to Alexa Fluor 488 (a2NTD-AF488) alone, or a2NTD-AF488 after the indicated inhibitors. Cell populations were analyzed by flow cytometry, upon gating on CD14⁺ event. (B and C) PBMCs were pre-treated with actin and microtubule inhibitors for 1 h followed by the exposure to 10 μ g/mL a2NTD-AF488 for 1 h. Representative histograms for each inhibitor are shown in (B). Dashed line depicts cells incubated with a2NTD-AF488 alone, while solid lines refer to cells exposed to inhibitors plus a2NTD. (C) Bar graph values in C illustrate the percentage of a2NTD-positive cells after inhibitor treatment. (means \pm SEM, n = 5, **p < 0.001, compared with a2NTD alone). (D) PBMCs were cultured in glucose-free media with or without NaN₃ and 2-deoxyglucose (to deplete ATP) or mycophenolic acid (to deplete GTP) for 2 h at 37°C, followed by the administration of a2NTD-AF488 for 1 h. Columns report mean fluorescence intensity (MFI) values (means \pm SEM, n = 5, *p < 0.05, compared with a2NTD alone).

than at 4°C (15%) (Fig. 1E). Cells were then treated with trypsin to remove any a2NTD bound to the cell surface. Thus, while trypsin reduced the number of a2NTD-positive cells in both temperature conditions, an increased number of fluorescent cells persisted at 37°C. Lymphocytes, which showed minimal binding to a2NTD, also exhibited minimal peptide uptake (Fig. 1E).

Endocytosis was confirmed by fluorescence microscopy. After incubation with fluorescent a2NTD, monocytes were examined by fluorescence microscopy, showing a2NTD-dependent surface staining at 4°C (Fig. 2A) and a more intense and intracellular punctate staining at 37°C (Fig. 2C). Similar to what was observed with flow cytometry, trypsin-treated monocytes

with approximately 45% of CD14⁺⁺CD16⁻ monocytes. The CD14⁺CD16⁺⁺ population showed a a2NTD uptake profile similar to that of CD14⁺⁺CD16⁻ cells (Fig. 4A).

a2NTD stimulates IL-1 α and IL-1 β production. It has previously been shown that a2NTD stimulates monocytes to produce the pro-inflammatory cytokines IL-1 α and IL-1 β .^{17,18} We examined whether a particular subset of monocytes is responsible for the production of inflammatory cytokines following a2NTD stimulation. To this aim, monocytes were incubated with a2NTD and then stained for surface CD14 and CD16 expression, followed by staining for the intracellular cytokines IL-1 α , IL-1 β and TNF- α .

Only CD14⁺⁺CD16⁺ monocytes showed a statistically significant increase in IL-1 α production when compared with cells maintained in control conditions (Fig. 4B). Both CD14⁺⁺CD16⁻ and CD14⁺⁺CD16⁺ monocytes produced significantly higher amounts of IL-1 β (Fig. 4C). There was no significant difference in the production of TNF α by cells treated with a2NTD and control cells (Fig. 4D). Of note, the CD14⁺⁺CD16⁺ subpopulation invariably produced higher amounts of IL-1 α , IL-1 β and TNF α than the other two subpopulations. In addition, the intracellular levels of IL-1 α and IL-1 β were greater than those of TNF α . This finding is consistent with our previous data demonstrating that monocytes produce more IL-1 than TNF.¹⁶ LPS contamination of the recombinant peptide is always a concern when investigating inflammatory cytokines. A multi-experimental approach was used to investigate the presence of LPS contamination, including the *Limulus* assay and polymyxin B neutralization tests. The results (which have previously been published) demonstrated negligible levels of LPS and that cytokine secretion could not be inhibited by pre-treatment with polymyxin B.¹⁶

Endocytosis of a2NTD occurs via macropinocytosis. To study the mechanism by which a2NTD is internalized, we examined three common pathways of cellular entry: clathrin-mediated endocytosis, caveolin-mediated endocytosis and macropinocytosis.²⁶ To this aim, PBMCs were pre-treated with distinct compounds that inhibit each of these pathways, followed by incubation with a2NTD. Chlorpromazine (CPZ) and dynasore were used to inhibit clathrin-mediated endocytosis. Neither of these inhibitors had an effect on a2NTD uptake (Fig. 5A). Filipin and nystatin were used to inhibit caveolin-mediated endocytosis. Similar to the inhibitors of clathrin-mediated endocytosis, filipin and nystatin did not affect a2NTD entry (Fig. 5B). Rottlerin and dimethylamiloride (DMA) were used to inhibit macropinocytosis. In contrast to the other inhibitors, both DMA and rottlerin significantly inhibited the uptake of a2NTD. In particular, rottlerin inhibited a2NTD uptake by 63% and DMA by 83% (Fig. 5C).

Table 1. Monocyte subtype percentages

Phenotype (Parent population)	Percent of parent population
CD14 ⁺ (PBMc)	6.96 \pm 1.5
CD14 ⁺⁺ CD16 ⁻ (CD14 ⁺ cells)	86.9 \pm 2.9
CD14 ⁺⁺ CD16 ⁺ (CD14 ⁺ cells)	5.5 \pm 1.2
CD14 ⁺ CD16 ⁺⁺ (CD14 ⁺ cells)	7.6 \pm 1.4

N = 10 mean \pm SEM.

To determine if a2NTD enhances macropinocytosis, PBMCs were incubated with a fluid-phase macropinocytosis marker, 10 kDa neutral dextran, in combination with increasing concentrations of a2NTD. Consistent with the observation of others,²⁷ dextran was efficiently taken up by macropinocytosis at 37°C. Of note, a2NTD induced a significant dose-dependent increase in the uptake of fluid-phase dextran (Fig. 5D). DMA pre-treatment significantly reduced dextran internalization as triggered by a2NTD. As THP-1 cells exhibited slower kinetics of a2NTD uptake, we investigated whether THP-1 cells bear a defective macropinocytosis machinery. When THP-1 cells were incubated with fluorescence 10 kDa dextran, cell fluorescence at 37°C

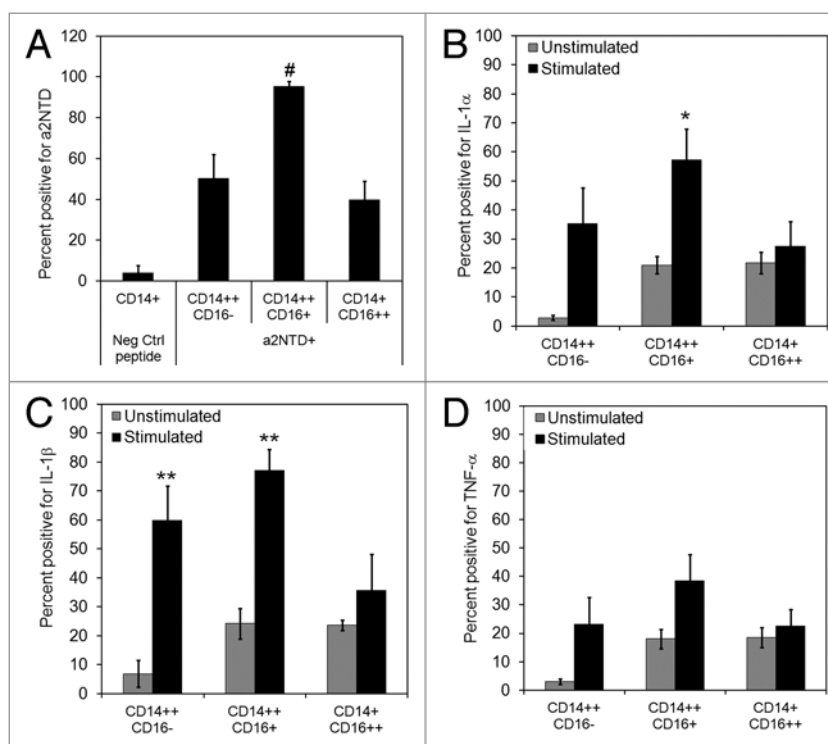


Figure 4. Binding of a2NTD and intracellular cytokine production in monocyte subpopulations. (A–D) Peripheral blood mononuclear cells (PBMCs) were incubated with 10 μ g/mL a2NTD conjugated to Alexa Fluor 488 (a2NTD-AF488) for 1 h and then surface stained with anti-CD14-Pacific Blue and anti-CD16-PE antibodies. (A) Percentage of monocyte populations positive for a2NTD-AF488. (means \pm SEM, n = 10, # p < 0.005, CD14⁺⁺CD16⁺ vs. CD14⁺⁺CD16⁻ or CD14⁺CD16⁺⁺ cells). (B–D) PBMCs were kept in control conditions or stimulated with 10 ng/mL a2NTD for 18 h and sequentially stained for surface expression of CD14/CD16 and the intracellular expression of interleukin (IL)-1 α : (B), IL-1 β (C) and tumor necrosis factor α (TNF α). (D) The bar graph reports the percentage of a2NTD-positive cells. (means \pm SEM, n = 5, *p < 0.05, **p < 0.001, compared with unstimulated cells of the same subpopulation).

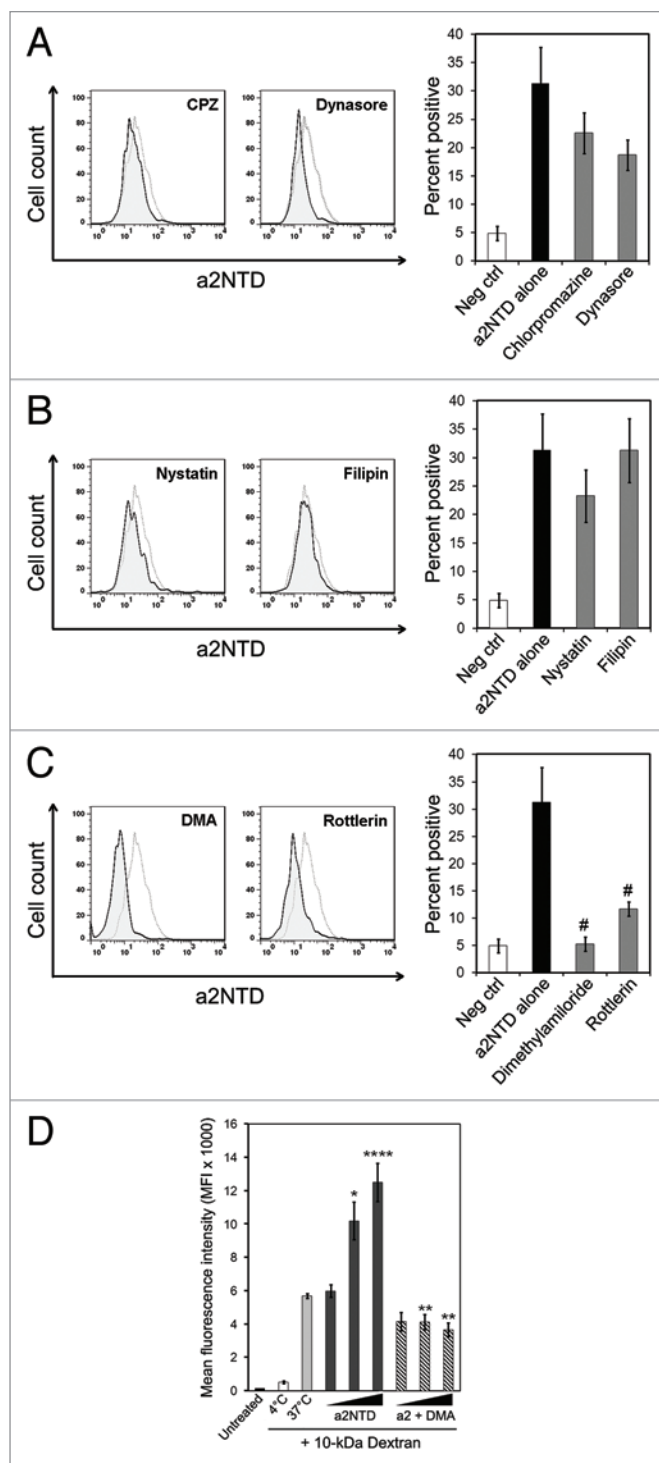


Figure 5. Inhibition of a2NTD endocytosis via trafficking inhibitors. (A–C) Peripheral blood mononuclear cells (PBMCs) were pre-incubated with the indicated trafficking inhibitors for 1 h at 37°C followed by the administration of 10 µg/mL a2NTD conjugated to Alexa Fluor 488 (a2NTD-AF488) for 1 additional h. Cell populations were analyzed by flow cytometry, upon gating on CD14⁺ events. Representative histograms for each trafficking inhibitor are reported. Dashed lines refer to cells incubated with a2NTD-AF488 alone, while solid lines depict cells incubated with trafficking inhibitor plus a2NTD. Bar graphs depict a2NTD-positive cells for clathrin-mediated endocytosis inhibitors (A), caveolin-mediated endocytosis inhibitors (B) and macropinocytosis inhibitors (C) (means ± SEM, n = 8, #p < 0.001, compared with a2NTD alone). (D) PBMCs were preincubated at 4°C or 37°C with 50 µg/mL 10 kDa dextran conjugated to Alexa Fluor 647 for 30 min. Some of the samples also received dimethylamiloride (DMA) for 30 min. Unconjugated a2NTD was then added (1–100 ng/mL) for 1 h at 37°C, followed by flow cytometry for the quantification of dextran-associated fluorescence. Columns report mean fluorescence intensity (MFI) values (means ± SEM, n = 4, *p < 0.01, ***p < 0.001, compared with cells maintained at 37°C, **p < 0.001, compared with cells receiving the same amount of a2NTD without DMA).

unknown. There is evidence suggesting that scavenger receptors utilize macropinocytosis as one mode of cellular entry.^{29,30} Scavenger receptors recognize macromolecules with negative charges³¹ as well as lipoproteins.³² Previous findings indicate that a2NTD is associated with lipids³³ and the amino acid sequence of a2NTD carries a net negative charge. We therefore examined whether scavenger receptors play a part in the endocytosis of a2NTD.

Polyinosinic acid (polyI), a polyanionic nucleotide, is a commonly used scavenger receptor ligand. PBMCs were pre-treated with polyanionic inhibitors before the addition of a2NTD and polyI significantly reduced a2NTD uptake by 80%, as compared with untreated samples (Fig. 6A). Polyadenylic acid and polycytidylic acid, structural homologs of polyI, did not inhibit a2NTD uptake.

Endocytosis is not required for cytokine production by a2NTD. We have previously shown a2NTD to upregulate the production of pro-inflammatory cytokines. We wanted then to determine if the internalization of a2NTD is required for cytokine production or if a2NTD binding is sufficient. After pre-incubation with trafficking inhibitors and a2NTD stimulation, monocytes were stained for intracellular IL-1β. None of the inhibitors had a statistically significant effect on IL-1β production (Fig. 6B). This indicates that the binding of a2NTD to monocytes is sufficient to stimulate a pro-inflammatory secretory response.

Discussion

TAMs are considered critical perpetrators of the low grade inflammation that is required to maintain tumor survival. The a2NTD peptide has been shown to stimulate monocytes to produce pro-inflammatory cytokines.^{17,18} In addition, a2NTD induces the expression of cytokines linked to M2 TAMs, which help in preventing immune cells from recognizing tumors.

To further characterize the interaction between monocytes and a2NTD, we are interested in determining the receptor(s)

increased similar to that of monocytes. The macropinocytotic response of THP-1 cells was also sensitive to DMA. However, while the co-administration of a2NTD slightly increased dextran uptake by THP-1 cells, this was not significant (Fig. S2B). Overall, the fluorescence intensity of dextran-treated THP-1 cells were 67% less than that of monocytes.

a2NTD uptake occurs via scavenger receptors. Scavenger receptors are recognized as key components of the innate immune system,²⁸ but the mechanism by which they signal remains

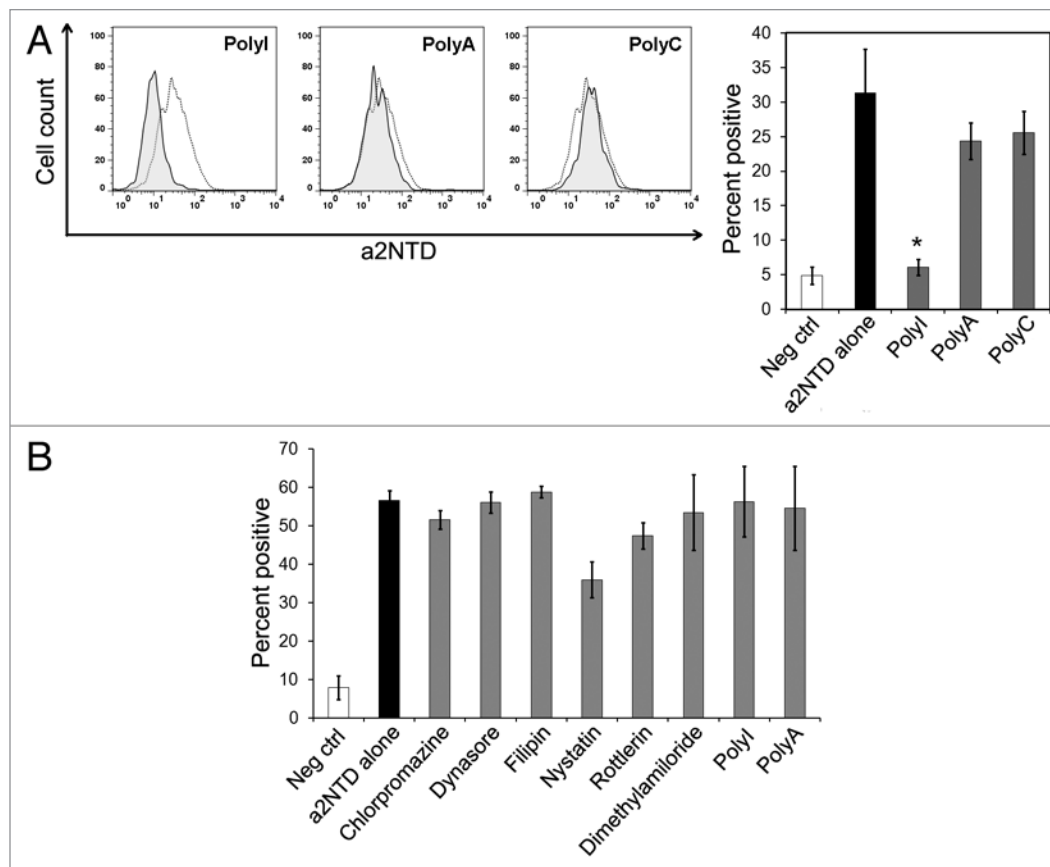


Figure 6. Inhibition of a2NTD endocytosis by scavenger receptor inhibitors. **(A and B)** Peripheral blood mononuclear cells (PBMCs) were pre-incubated with the indicated inhibitors for 1 h at 37°C followed by incubation with 10 μ g/mL a2NTD conjugated to Alexa Fluor 488 (a2NTD-AF488) for 1 h. Cell populations were analyzed by flow cytometry, upon gating on CD14⁺ events. Representative histograms for each inhibitor or negative control are shown. Dashed lines refer to a2NTD-AF488 alone, solid lines to scavenger receptor inhibitors or negative controls plus a2NTD. Columns depict the percentage of a2NTD-positive cells (means \pm SEM, $n = 8$, * $p < 0.001$, compared with a2NTD alone). **(B)** PBMCs were pre-incubated with indicated trafficking inhibitors for 1 h followed by incubation with unconjugated a2NTD for 18 h. Cells were then stained for surface CD14 and then for intracellular interleukin (IL)-1 β . Cell populations were analyzed by flow cytometry, upon gating on CD14⁺ events. Columns depict the percentage of a2NTD-positive cells (means \pm SEM, $n = 5$).

that interacts with a2NTD. While a2NTD binds to the cell surface and enters both monocytes and THP-1 cells, the former bind higher amounts of a2NTD and internalize the peptide at a much faster pace than the latter (Fig. 1E and Fig. S2A). This would suggest that THP-1 cells may express reduced amounts of the proteins that are necessary for a2NTD binding and internalization.

Our previous studies have shown that a2NTD stimulates both monocytes and THP-1 cells to produce IL-1 β . However, only monocytes (but not THP-1 cells) generate reactive oxygen species (ROS) upon a2NTD stimulation.¹⁶ This is consistent with the concept that THP-1 cells express less or lack some of the proteins that mediate the endocytosis of a2NTD. Monocytes stimulated with a2NTD in the presence of trafficking inhibitors produced pro-inflammatory cytokines, indicating that the entry of a2NTD is not necessary for cytokine production (Fig. 6B). Taken together, these data suggest a possible dual receptor process. Thus, while both monocytes and THP-1 cells appear to express the a2NTD receptor that is important for IL-1 β secretion, only monocytes have a second receptor that brings a2NTD into the cell and leads to intracellular ROS production. In monocytes,

ROS may be a redundant amplification signal to produce additional inflammatory cytokines. THP-1 cells seem not to express this putative receptor to sufficient levels and thus cannot produce ROS in response to a2NTD.

The inhibition of a2NTD endocytosis with polyI (Fig. 6A) indicates that a scavenger receptor is involved in a2NTD internalization. Scavenger receptors are a broad family of integral membrane proteins that mediate the cellular binding and internalization of an extraordinarily wide range of negatively charged macromolecules including lipoproteins,³⁴ polyribonucleotides (such as polyI)³⁵ and advanced-glycation end products.³⁶ Macrophages have been well characterized in their expression of scavenger receptors, especially linked to their pathological role in atherosclerotic plaques.³⁷ The a2NTD peptide carries a net negative charge at physiological pH. In addition, the a2 N-terminal domain exhibits physicochemical properties that are compatible with its integration in membranes.³³ Hence, it is not surprising that scavenger receptors would mediate the endocytosis of a2NTD.

CD14⁺CD16⁻ monocytes have been shown to be generally more phagocytic than their CD14⁺CD16⁺ counterparts.³⁸

Here, we demonstrate a preferential uptake of a2NTD by CD14⁺⁺CD16⁺, suggesting that a relatively specific process is taking place as opposed to unspecific phagocytosis. We have previously implicated a2NTD in promoting the development of a TAM phenotype and CD14⁺CD16⁺ monocytes are thought to constitute macrophage precursors.¹⁵ This is another piece of evidence indicating the internalization of a2NTD is a specific receptor-mediated process.

An interesting finding is the characterization of the monocyte subsets that produce cytokines in response to a2NTD stimulation. CD14⁺CD16⁺ monocytes have previously been characterized as the main producers of pro-inflammatory cytokines^{39,40} in an LPS stimulation model. However, both CD14⁺⁺CD16⁻ and CD14⁺⁺CD16⁺ monocytes produce significant amounts of IL-1 in response to a2NTD (Fig. 4). CD14⁺CD16⁺ monocytes are also a major source of TNF α upon LPS stimulation.⁴¹ In contrast, there is no significant TNF α production after the administration of a2NTD to these cells. Previous data indicate that the production of IL-1 is privileged over that of TNF α after a2NTD stimulation. The data presented here are consistent with these findings. While CD14⁺CD16⁺ monocytes have been extensively studied for their role in infectious diseases and inflammation,⁴² their role in tumorigenesis has only recently been explored.^{43,44} The interaction of CD14⁺⁺CD16⁻ monocytes with a2NTD, stimulating the production of pro-inflammatory cytokines represents a new area of research for how the monocyte subsets are functionally defined.

In summary, the a2NTD peptide may play a prominent role in the tumor microenvironment. While functioning to promote a localized pro-inflammatory reaction, a2NTD also prevents immune surveillance, and the interaction of a2NTD with specific monocyte subsets appears to stimulate their pro-tumorigenic functions. Our data indicate there is more than one cell type responding to a2NTD. Identifying the receptor(s) of a2NTD as well as understanding the differences among different types of a2NTD-sensitive cells will perhaps drive the development of novel anticancer therapies.

Materials and Methods

Reagents and antibodies. Recombinant a2NTD was expressed and purified from *Escherichia coli* and subjected to endotoxin removal column chromatography (Proteome Resources). Recombinant a2NTD was conjugated to Alexa Fluor 488 (a2NTD-AF488) via a microscale labeling kit (Invitrogen, A30006). Conjugation of a2NTD to AF488 was kept within a range of 1–3 mol of dye per mol of a2NTD. A scrambled peptide conjugated to FITC was used as a negative control.

Lipopolysaccharide (L6529), chlorpromazine (C8138), filipin (F9765), rottlerin (R5648), polyinosinic acid (P4154), polycytidylic acid (P4903), polyadenylic acid (P9403), nystatin (N4014), dimethylamiloride (A4562), cytochalasin D (C2618), dynasore (D7693), 2-deoxy-D-glucose (D1634), sodium azide (71289), colchicine (C3915) and mycophenolic acid (M3563) were purchased from Sigma Aldrich. Paraformaldehyde ampules were from Thermo Scientific (PI28908). Anti-CD14

PE-Texas Red was from Invitrogen (HCD1417C). Anti-CD14 PE (555398), anti-CD16 Pacific Blue (558122), anti-IL-1 α FITC (340513), anti-IL-1 β FITC (340515), anti-TNF α FITC (340511), mouse IgG2a PE (555574), mouse IgG1 Pacific Blue (558120), mouse IgG1 FITC (555909) were from Becton Dickinson.

Mononuclear isolation and cell culture. These studies were approved by the University institutional review board. After informed consent was obtained in accordance with the Declaration of Helsinki, peripheral blood was collected into sodium heparin vacutainers (Thermo Fisher, 026853B). The peripheral blood mononuclear cell (PBMC) fraction was collected after differential density centrifugation over Ficoll-Paque PLUS (Thermo Fisher, 45-001-750). The human monocytic leukemia cell line THP-1 was purchased from ATCC (TIB-202) and maintained in RPMI 1640 medium (ATCC, 30-2001) supplemented with 10% fetal bovine serum and 1 \times antibiotic/antimycotic solution (Invitrogen, 15240096) at 37°C with 5% CO₂. Routine mycoplasma testing was conducted using the MycoAlert assay from Lonza (LT07-318, LT07-518). A concentration of 1 \times 10⁶ PBMCs or THP-1 cells was used for all experiments.

Flow cytometry. All samples analyzed by flow cytometry were run on an LSRII flow cytometer (Becton Dickinson). FlowJo software was used for data analysis (TreeStar).

Fluorescence microscopy. A Shandon cytospin 2 (Thermo Scientific) was used to spin stained cells onto microscope slides. The ProLong Gold antifade reagent with DAPI (Invitrogen, P-36935) was used as mounting medium and slides were left overnight at room temperature to allow mounting media to fix. Slides were visualized with a Nikon Eclipse 80i fluorescence microscope and images were acquired with a Photometrics CoolSNAP ES camera. Metamorph software (Molecular Devices) was used for analysis. Adobe Photoshop version CS2 was used for figure arrangement.

Dose and competition assay. PBMCs were fixed in 2% paraformaldehyde (PFA) for 15 min and washed twice in PBS. Cells were then incubated with a2NTD-AF488 at the indicated concentrations for 1 h on ice to prevent endocytosis. For competition assays, cells were incubated with unconjugated a2NTD for 1 h at increasing concentrations. Conjugated 20 μ g/mL a2NTD was then added for 1 h on ice. For both assays, cells were washed twice in PBS after incubations before analyzing via flow cytometry.

Time and temperature assays. Unfixed PBMCs were incubated with 10 μ g/mL a2NTD-AF488 for indicated time points at 37°C or 4°C. Half the samples were then treated with 0.1% trypsin-EDTA (Sigma Aldrich T-4049) for 5 min at room temperature to remove surface bound a2NTD followed by two washes in PBS. Cells were stained with anti-CD14 Pacific Blue for 30 min on ice and then washed followed by fixation with 2% PFA. Samples were then analyzed by flow cytometry or fluorescence microscopy.

ATP and GTP depletion assay. PBMCs were incubated in glucose-free RPMI medium (Invitrogen, 11879-020) with 8 mM 2-deoxy-glucose⁴⁵ and 20 mM sodium azide⁴⁵ (to deplete ATP) or 0.5 μ g/mL mycophenolic acid⁴⁶ (to deplete GTP) for 2 h at

37°C. Ten µg/mL a2NTD-AF488 was then added for an additional 1 h at 37°C. Cells were washed twice in PBS and analyzed by flow cytometry.

Immunophenotyping and intracellular cytokine staining. PBMCs were incubated with 10 µg/mL a2NTD-AF488 for 1 h on ice. Cells were then incubated with anti-CD14 Pacific Blue and anti-CD16 PE antibodies for 15 min at 4°C, washed twice with PBS and analyzed by flow cytometry. For intracellular cytokine staining, PBMCs were stimulated with 100 ng/mL unconjugated a2NTD for 18 h with the trafficking inhibitor GolgiPlug (Becton Dickinson, 555029) which contains brefeldin A. Cells were then stained with anti-CD14 and anti-CD16 antibodies as described above. After incubating with the Cytofix/Cytoperm reagent (Becton Dickinson, 554722) for 20 min at 4°C, cells were washed twice in Perm/Wash reagent (Becton Dickinson, 554723) and then incubated with anti-IL-1α-FITC, IL-1β-FITC, TNFα-FITC, or equivalent isotype antibodies for 30 min at 4°C. Cells were then washed twice with Perm/Wash and analyzed by flow cytometry.

Trafficking inhibition. PBMCs were pre-incubated with trafficking inhibitors for 1 h at 37°C at the following concentrations: 20 µM chlorpromazine,⁴⁷ 80 µM dynasore,⁴⁸ 2 µg/mL filipin,⁴⁹ 20 µg/mL nystatin,⁴⁹ 10 µM rottlerin,⁴⁹ 500 µM dimethylamiloride,⁵⁰ 50 µg/mL polyinosinic acid,⁵⁰ 50 µg/mL polyadenylic acid,⁵¹ 50 µg/mL polycytidylic acid,⁵¹ 2.5 µg/mL cytochalasin D⁴⁹ and 50 µg/mL colchicine.⁵² 10 µg/mL a2NTD-AF488 was then added for 1 h at 37°C to allow for endocytosis. Some samples were incubated with unconjugated a2NTD and inhibitors for 18 h and then stained for intracellular cytokines as described above. Cells were then stained with anti-CD14 Pacific Blue for 30 min on ice, washed twice with PBS and analyzed by flow cytometry or fluorescence microscopy.

Ten kDa dextran uptake assay. To measure the effects of a2NTD on macropinocytosis, PBMCs were incubated with 50 µg/mL 10 kDa neutral dextran Alexa Fluor 647 (Invitrogen,

D22914) and 0.1 ng/mL, 1.0 ng/mL, or 10 ng/mL a2NTD for 1 h at 4°C or 37°C. To confirm that macropinocytosis was taking place, cells were pre-incubated with dimethylamiloride for 30 min at 37°C and then treated with 10 kDa neutral dextran Alexa Fluor 647. To remove surface bound dextran, cells were treated with 0.1% trypsin-EDTA and the cells were then fixed in 2% PFA followed by two washes in PBS and then analyzed by flow cytometry.

Cell viability and cytotoxicity assays. PBMCs and primary monocytes were incubated with different concentrations of trafficking inhibitors for indicated times. Cell viability was measured via two different assays: an ATP (G7570) and a NADH assay (G8080). Cellular toxicity was measured by using a live vs. dead cell proteases assay (G9201). All three kits were conducted following the manufacturer's instructions (Promega). Digitonin, a detergent, was used as a positive control (Sigma, D141).

Statistical analyses. The Student's paired t-test was used to compare two groups. If more than two groups were being compared, repeated measures ANOVA was applied. Results are reported as means ± SEM and significance was defined as indicated in figure legends. Results were analyzed using Sigma Plot 11 (Systat Software Inc.).

Disclosure of Potential Conflicts of Interest

The authors declare no competing financial interests.

Acknowledgments

We thank Rita Levine and Robert Dickinson for their assistance with fluorescence-activated cell sorter analysis at the flow cytometry core facility at Rosalind Franklin University of Medicine and Science.

Supplemental Materials

Supplemental materials may be found here: www.landesbioscience.com/journals/oncoimmunology/article/22978

References

1. Sennoune SR, Luo D, Martínez-Zaguilán R. Plasmalemmal vacuolar-type H⁺-ATPase in cancer biology. *Cell Biochem Biophys* 2004; 40:185-206; PMID:15054222; <http://dx.doi.org/10.1385/CBB:40:2:185>.
2. Martínez-Zaguilán R, Lynch RM, Martínez GM, Gillies RJ. Vacuolar-type H⁺-ATPases are functionally expressed in plasma membranes of human tumor cells. *Am J Physiol* 1993; 265:C1015-29; PMID:8238296.
3. Kubota S, Seyama Y. Overexpression of vacuolar ATPase 16-kDa subunit in 10T1/2 fibroblasts enhances invasion with concomitant induction of matrix metalloproteinase-2. *Biochem Biophys Res Commun* 2000; 278:390-4; PMID:11097847; <http://dx.doi.org/10.1006/bbrc.2000.3802>.
4. Rofstad EK, Mathiesen B, Kindem K, Galappathi K. Acidic extracellular pH promotes experimental metastasis of human melanoma cells in athymic nude mice. *Cancer Res* 2006; 66:6699-707; PMID:16818644; <http://dx.doi.org/10.1158/0008-5472.CAN-06-0983>.
5. Sennoune SR, Bakunts K, Martínez GM, Chua-Tuan JL, Kebir Y, Attaya MN, et al. Vacuolar H⁺-ATPase in human breast cancer cells with distinct metastatic potential: distribution and functional activity. *Am J Physiol Cell Physiol* 2004; 286:C1443-52; PMID:14761893; <http://dx.doi.org/10.1152/ajpcell.00407.2003>.
6. Mantovani A, Sozzani S, Locati M, Allavena P, Sica A. Macrophage polarization: tumor-associated macrophages as a paradigm for polarized M2 mononuclear phagocytes. *Trends Immunol* 2002; 23:549-55; PMID:12401408; [http://dx.doi.org/10.1016/S1471-4906\(02\)02302-5](http://dx.doi.org/10.1016/S1471-4906(02)02302-5).
7. Cortez-Retamozo V, Etzrodt M, Newton A, Rauch PJ, Chudnovskiy A, Berger C, et al. Origins of tumor-associated macrophages and neutrophils. *Proc Natl Acad Sci U S A* 2012; 109:2491-6; PMID:22308361; <http://dx.doi.org/10.1073/pnas.1113744109>.
8. Stein M, Keshav S, Harris N, Gordon S. Interleukin 4 potentially enhances murine macrophage mannose receptor activity: a marker of alternative immunologic macrophage activation. *J Exp Med* 1992; 176:287-92; PMID:1613462; <http://dx.doi.org/10.1084/jem.176.1.287>.
9. Goerdt S, Orfanos CE. Other functions, other genes: alternative activation of antigen-presenting cells. *Immunity* 1999; 10:137-42; PMID:10072066; [http://dx.doi.org/10.1016/S1074-7613\(00\)80014-X](http://dx.doi.org/10.1016/S1074-7613(00)80014-X).
10. Wyckoff J, Wang W, Lin EY, Wang Y, Pixley F, Stanley ER, et al. A paracrine loop between tumor cells and macrophages is required for tumor cell migration in mammary tumors. *Cancer Res* 2004; 64:7022-9; PMID:15466195; <http://dx.doi.org/10.1158/0008-5472.CAN-04-1449>.
11. Albini A, Tosetti F, Benelli R, Noonan DM. Tumor inflammatory angiogenesis and its chemoprevention. *Cancer Res* 2005; 65:10637-41; PMID:16322203; <http://dx.doi.org/10.1158/0008-5472.CAN-05-3473>.
12. Wynn TA. Fibrotic disease and the T(H)1/T(H)2 paradigm. *Nat Rev Immunol* 2004; 4:583-94; PMID:15286725; <http://dx.doi.org/10.1038/nri1412>.
13. Mantovani A, Sica A, Sozzani S, Allavena P, Vecchi A, Locati M. The chemokine system in diverse forms of macrophage activation and polarization. *Trends Immunol* 2004; 25:677-86; PMID:15530839; <http://dx.doi.org/10.1016/j.it.2004.09.015>.
14. Ziegler-Heitbrock L, Ancuta P, Crowe S, Dalod M, Grau V, Hart DN, et al. Nomenclature of monocytes and dendritic cells in blood. *Blood* 2010; 116:e74-80; PMID:20628149; <http://dx.doi.org/10.1182/blood-2010-02-258558>.
15. Almeida J, Bueno C, Algueró MC, Sanchez ML, de Santiago M, Escribano L, et al. Comparative analysis of the morphological, cytochemical, immunophenotypic, and functional characteristics of normal human peripheral blood lineage(-)/CD16(+)/HLA-DR(+)/CD14(-/lo) cells, CD14(+) monocytes, and CD16(-) dendritic cells. *Clin Immunol* 2001; 100:325-38; PMID:11513546; <http://dx.doi.org/10.1006/clim.2001.5072>.

16. Kwong C, Gilman-Sachs A, Beaman K. Tumor-associated $\alpha 2$ vacuolar ATPase acts as a key mediator of cancer-related inflammation by inducing protumorigenic properties in monocytes. *J Immunol* 2011; 186:1781-9; PMID:21178005; <http://dx.doi.org/10.4049/jimmunol.1002998>.
17. Ntrivalas E, Gilman-Sachs A, Kwak-Kim J, Beaman K. The N-terminus domain of the $\alpha 2$ isoform of vacuolar ATPase can regulate interleukin-1 β production from mononuclear cells in co-culture with JEG-3 choriocarcinoma cells. *Am J Reprod Immunol* 2007; 57:201-9; PMID:17295899; <http://dx.doi.org/10.1111/j.1600-0897.2006.00463.x>.
18. Ntrivalas E, Derks R, Gilman-Sachs A, Kwak-Kim J, Levine R, Beaman K. Novel role for the N-terminus domain of the $\alpha 2$ isoform of vacuolar ATPase in interleukin-1 β production. *Hum Immunol* 2007; 68:469-77; PMID:17509446; <http://dx.doi.org/10.1016/j.humimm.2007.02.010>.
19. Gürsoy RN, Siahaan TJ. Binding and internalization of an ICAM-1 peptide by the surface receptors of T cells. *J Pept Res* 1999; 53:414-21; PMID:10406219; <http://dx.doi.org/10.1034/j.1399-3011.1999.00079.x>.
20. Apodaca G. Endocytic traffic in polarized epithelial cells: role of the actin and microtubule cytoskeleton. *Traffic* 2001; 2:149-59; PMID:11260520; <http://dx.doi.org/10.1034/j.1600-0854.2001.020301.x>.
21. Newman SL, Mikus LK, Tucci MA. Differential requirements for cellular cytoskeleton in human macrophage complement receptor- and Fc receptor-mediated phagocytosis. *J Immunol* 1991; 146:967-74; PMID:1846386.
22. Allen LA, Aderem A. Molecular definition of distinct cytoskeletal structures involved in complement- and Fc receptor-mediated phagocytosis in macrophages. *J Exp Med* 1996; 184:627-37; PMID:8760816; <http://dx.doi.org/10.1084/jem.184.2.627>.
23. Gekle M, Mildnerberger S, Freudinger R, Schwerdt G, Silbernagl S. Albumin endocytosis in OK cells: dependence on actin and microtubules and regulation by protein kinases. *Am J Physiol* 1997; 272:F668-77; PMID:9176379.
24. Piasek A, Thyberg J. Effects of colchicine on endocytosis of horseradish peroxidase by rat peritoneal macrophages. *J Cell Sci* 1980; 45:59-71; PMID:7462349.
25. Wong KL, Tai JJ, Wong WC, Han H, Sem X, Yeap WH, et al. Gene expression profiling reveals the defining features of the classical, intermediate, and nonclassical human monocyte subsets. *Blood* 2011; 118:e16-31; PMID:21653326; <http://dx.doi.org/10.1182/blood-2010-12-326355>.
26. Doherty GJ, McMahon HT. Mechanisms of endocytosis. *Annu Rev Biochem* 2009; 78:857-902; PMID:19317650; <http://dx.doi.org/10.1146/annurev.biochem.78.081307.110540>.
27. Araki N, Johnson MT, Swanson JA. A role for phosphoinositide 3-kinase in the completion of macropinocytosis and phagocytosis by macrophages. *J Cell Biol* 1996; 135:1249-60; PMID:8947549; <http://dx.doi.org/10.1083/jcb.135.5.1249>.
28. Areschoug T, Gordon S. Scavenger receptors: role in innate immunity and microbial pathogenesis. *Cell Microbiol* 2009; 11:1160-9; PMID:19388903; <http://dx.doi.org/10.1111/j.1462-5822.2009.01326.x>.
29. Sulhian TH, Imrich A, Deloid G, Winkler AR, Kobzik L. Signaling pathways required for macrophage scavenger receptor-mediated phagocytosis: analysis by scanning cytometry. *Respir Res* 2008; 9:59; PMID:18687123; <http://dx.doi.org/10.1186/1465-9921-9-59>.
30. Yao W, Li K, Liao K. Macropinocytosis contributes to the macrophage foam cell formation in RAW264.7 cells. *Acta Biochim Biophys Sin (Shanghai)* 2009; 41:773-80; PMID:19727526; <http://dx.doi.org/10.1093/abbs/gmp066>.
31. Greenberg JW, Fischer W, Joiner KA. Influence of lipoteichoic acid structure on recognition by the macrophage scavenger receptor. *Infect Immun* 1996; 64:3318-25; PMID:8757870.
32. Matsumoto A, Naito M, Itakura H, Ikemoto S, Asaoka H, Hayakawa I, et al. Human macrophage scavenger receptors: primary structure, expression, and localization in atherosclerotic lesions. *Proc Natl Acad Sci U S A* 1990; 87:9133-7; PMID:2251254; <http://dx.doi.org/10.1073/pnas.87.23.9133>.
33. Merkulova M, McKee M, Dip PV, Grüber G, Marshansky V. N-terminal domain of the V-ATPase $\alpha 2$ -subunit displays integral membrane protein properties. *Protein Sci* 2010; 19:1850-62; PMID:20669186; <http://dx.doi.org/10.1002/pro.470>.
34. Steinbrecher UP, Loughheed M, Kwan WC, Dirks M. Recognition of oxidized low density lipoprotein by the scavenger receptor of macrophages results from derivatization of apolipoprotein B by products of fatty acid peroxidation. *J Biol Chem* 1989; 264:15216-23; PMID:2768257.
35. Brown MS, Basu SK, Falck JR, Ho YK, Goldstein JL. The scavenger cell pathway for lipoprotein degradation: specificity of the binding site that mediates the uptake of negatively-charged LDL by macrophages. *J Supramol Struct* 1980; 13:67-81; PMID:6255257; <http://dx.doi.org/10.1002/jss.400130107>.
36. Araki N, Higashi T, Mori T, Shibayama R, Kawabe Y, Kodama T, et al. Macrophage scavenger receptor mediates the endocytic uptake and degradation of advanced glycation end products of the Maillard reaction. *Eur J Biochem* 1995; 230:408-15; PMID:7607209; <http://dx.doi.org/10.1111/j.1432-1033.1995.0408h.x>.
37. Freeman MW. Scavenger receptors in atherosclerosis. *Curr Opin Hematol* 1997; 4:41-7; PMID:9050378; <http://dx.doi.org/10.1097/00062752-199704010-00007>.
38. Auffray C, Sieweke MH, Geissmann F. Blood monocytes: development, heterogeneity, and relationship with dendritic cells. *Annu Rev Immunol* 2009; 27:669-92; PMID:19132917; <http://dx.doi.org/10.1146/annurev.immunol.021908.132557>.
39. Ziegler-Heitbrock HW. Heterogeneity of human blood monocytes: the CD14+ CD16+ subpopulation. *Immunol Today* 1996; 17:424-8; PMID:8854561; [http://dx.doi.org/10.1016/0167-5699\(96\)10029-3](http://dx.doi.org/10.1016/0167-5699(96)10029-3).
40. Ziegler-Heitbrock HW. Definition of human blood monocytes. *J Leukoc Biol* 2000; 67:603-6; PMID:10810998.
41. Belge KU, Dayyani F, Horelt A, Siedlar M, Frankenberger M, Frankenberger B, et al. The pro-inflammatory CD14+CD16+DR++ monocytes are a major source of TNF. *J Immunol* 2002; 168:3536-42; PMID:11907116.
42. Ziegler-Heitbrock L. The CD14+ CD16+ blood monocytes: their role in infection and inflammation. *J Leukoc Biol* 2007; 81:584-92; PMID:17135573; <http://dx.doi.org/10.1189/jlb.0806510>.
43. De Palma M, Murdoch C, Venneri MA, Naldini L, Lewis CE. Tie2-expressing monocytes: regulation of tumor angiogenesis and therapeutic implications. *Trends Immunol* 2007; 28:519-24; PMID:17981504; <http://dx.doi.org/10.1016/j.it.2007.09.004>.
44. Subimerb C, Pinlaor S, Lulitanond V, Khuntikeo N, Okada S, McGrath MS, et al. Circulating CD14(+) CD16(+) monocyte levels predict tissue invasive character of cholangiocarcinoma. *Clin Exp Immunol* 2010; 161:471-9; PMID:20636398; <http://dx.doi.org/10.1111/j.1365-2249.2010.04200.x>.
45. Nishimura S, Takahashi S, Kamikatahira H, Kuroki Y, Jaalouk DE, O'Brien S, et al. Combinatorial targeting of the macropinocytotic pathway in leukemia and lymphoma cells. *J Biol Chem* 2008; 283:11752-62; PMID:18292083; <http://dx.doi.org/10.1074/jbc.M708849200>.
46. Chaigne-Delalande B, Guidicelli G, Couzi L, Merville P, Mahfouf W, Bouchet S, et al. The immunosuppressor mycophenolic acid kills activated lymphocytes by inducing a nonclassical actin-dependent necrotic signal. *J Immunol* 2008; 181:7630-8; PMID:19017951.
47. Inoue Y, Tanaka N, Tanaka Y, Inoue S, Morita K, Zhuang M, et al. Clathrin-dependent entry of severe acute respiratory syndrome coronavirus into target cells expressing ACE2 with the cytoplasmic tail deleted. *J Virol* 2007; 81:8722-9; PMID:17522231; <http://dx.doi.org/10.1128/JVI.00253-07>.
48. Macia E, Ehrlich M, Massol R, Boucrot E, Brunner C, Kirchhausen T. Dynasore, a cell-permeable inhibitor of dynamin. *Dev Cell* 2006; 10:839-50; PMID:16740485; <http://dx.doi.org/10.1016/j.devcel.2006.04.002>.
49. Raghu H, Sharma-Walia N, Veetil MV, Sadagopan S, Chandran B. Kaposi's sarcoma-associated herpesvirus utilizes an actin polymerization-dependent macropinocytic pathway to enter human dermal microvascular endothelial and human umbilical vein endothelial cells. *J Virol* 2009; 83:4895-911; PMID:19279100; <http://dx.doi.org/10.1128/JVI.02498-08>.
50. Burgdorf S, Kautz A, Böhnert V, Knolle PA, Kurts C. Distinct pathways of antigen uptake and intracellular routing in CD4 and CD8 T cell activation. *Science* 2007; 316:612-6; PMID:17463291; <http://dx.doi.org/10.1126/science.1137971>.
51. Dunzendorfer S, Lee HK, Soldau K, Tobias PS. TLR4 is the signaling but not the lipopolysaccharide uptake receptor. *J Immunol* 2004; 173:1166-70; PMID:15240706.
52. Kindzelskii AL, Huang JB, Chaiworapongsa T, Fahmy RM, Kim YM, Romero R, et al. Pregnancy alters glucose-6-phosphate dehydrogenase trafficking, cell metabolism, and oxidant release of maternal neutrophils. *J Clin Invest* 2002; 110:1801-11; PMID:12488430.